Regions of nonexistence of invariant tori for spin-orbit models

Alessandra Celletti[a)]
Dipartimento di Matematica, Università di Roma Tor Vergata, Via della Ricerca Scientifica 1, I-00133 Roma, Italy

Robert MacKay[b)]
Mathematics Institute, University of Warwick, Coventry CV4 7AL, United Kingdom

(Received 26 July 2007; accepted 17 October 2007; published online 26 November 2007)

The spin-orbit problem in celestial mechanics describes the motion of an oblate satellite moving on a Keplerian orbit around a primary body. We apply the conjugate points criterion for the nonexistence of rotational invariant tori. We treat both the conservative case and a case including a dissipative effect modeling a tidal torque generated by internal nonrigidity. As a by-product of the conjugate points criterion we obtain a global view of the dynamics, thanks to the introduction of a *tangent orbit indicator*, which allows us to discern the dynamical character of the motion. © *2007 American Institute of Physics*. [DOI: 10.1063/1.2811880]

Nearly integrable Hamiltonian systems admit rotational invariant tori (continuous deformations of those of the integrable case) when the perturbation is sufficiently small; indeed, Kolmogorov-Arnold-Moser (KAM) theory provides a lower bound on the perturbing parameter ensuring the existence of rotational invariant tori with given diophantine frequencies. On the other hand, they are all destroyed for systems sufficiently "far" from integrable: regions of parameter and phase space for which there are no rotational invariant tori can be obtained by converse KAM theory, as developed in Refs. 9–11. Among the techniques developed in the framework of converse KAM theory, we are principally concerned with the *conjugate points* criterion as described in Ref. 9. In this paper we discuss its application to a specific problem of celestial mechanics, namely the rotational dynamics of a triaxial satellite revolving on a Keplerian orbit around a primary body. We consider both rigid and nonrigid models, providing in each case a global view of their dynamics.

I. INTRODUCTION

Under some simplifying assumptions, the conservative (rigid) model is described by a one-dimensional, time-dependent differential equation. We consider also a truncation of the Taylor expansion in terms of the orbital eccentricity and of the Fourier-series development of the equation of motion (see, e.g., Ref. 2). Besides the above conservative model, we also consider the spin-orbit interaction of a nonrigid satellite; the tidal torque induced by the nonrigidity is modeled by the MacDonald torque (see Ref. 5 for a discussion of the tidal evolution and Ref. 3 for the existence of quasiperiodic attractors). Within the spin-orbit model, we are interested in the dynamics around resonances, which occur whenever the ratio of the periods of revolution and rotation is rational. For example, the Moon is observed to move in a synchronous resonance, since it makes one rotation during a full revolution. Most of the evolved satellites of the solar system are seen to move in a synchronous resonance; the only exception is provided by Mercury, whose astronomical measurements show that the planet completes three rotations during two revolutions around the Sun.

Using the above models, with application to the Moon or Mercury in mind, we implement the nonexistence criterion in the style of Ref. 9. We remark that the study of the behavior of a quantity related to this criterion, which we call the *tangent orbit indicator,* allows us to give a description of the dynamics, being able to discern between librational, rotational or chaotic motion, therefore providing a global view of the dynamics with high accuracy and within a reasonable computational effort.

II. THE SPIN-ORBIT MODEL

Let S be a triaxial satellite orbiting around a central planet, say P, and rotating about an internal spin-axis. A simple nontrivial model of spin-orbit interaction is obtained under the following assumptions (see, e.g., Ref. 2):

(i) the satellite is assumed to move on a Keplerian orbit around the planet;
(ii) the spin-axis coincides with the smallest physical axis (i.e., the axis of largest moment of inertia);
(iii) the spin-axis is assumed to be constantly perpendicular to the orbital plane.

A. The conservative model

The conservative model makes the additional assumption that one can neglect dissipative forces, most notably the tidal torque due to the internal nonrigidity of the satellite. With reference to the Keplerian orbit of the satellite, let us denote by a, r, f, the semimajor axis, the instantaneous orbital radius and the true anomaly. Let $A<B<C$ be the principal moments of inertia of the satellite; finally, let x be the

a)Electronic mail: celletti@mat.uniroma2.it.
b)Electronic mail: R.S.MacKay@warwick.ac.uk.

angle between the longest axis of the ellipsoid and the pericenter line. Normalizing to 1 the mean motion $n=2\pi/T_{\rm rev}$, the equation of motion is

$$\ddot{x}+\varepsilon\left(\frac{a}{r}\right)^3\sin(2x-2f)=0, \tag{1}$$

where the parameter

$$\varepsilon\equiv\frac{3}{2}\frac{B-A}{C}$$

is proportional to the equatorial oblateness of the satellite. If $A=B$ (equatorial symmetry), then $\varepsilon=0$ and the equation of motion is trivially integrable. The actual values of ε for the Moon and Mercury are given by $\varepsilon=3.45\times10^{-4}$ and $\varepsilon=1.5\times10^{-4}$.

By assumption (i), the orbital radius r and the true anomaly f are Keplerian functions of the time. They also depend on the orbital eccentricity e; in the limiting case of $e=0$ one obtains $r=a=$const and $f=t+$const. The dependence of r and f on time t can be obtained through the Keplerian relations involving the eccentric anomaly u,

$$\begin{aligned} r&=a(1-e\cos u),\\ f&=2\arctan\left(\sqrt{\frac{1+e}{1-e}}\tan\frac{u}{2}\right),\end{aligned} \tag{2}$$

where u is related to the mean anomaly $\ell=t+\ell_0$ (ℓ_0 is some initial condition on the mean anomaly) through Kepler's equation $\ell=u-e\sin u$.

A spin-orbit resonance of order p/q, for some integers p,q with $q>0$, is a solution $x=x(t)$ such that

$$\langle\dot{x}\rangle=\frac{p}{q},$$

which means that during q revolutions around the planet, the satellite makes on average p rotations about the spin-axis. In the case of a 1:1 spin-orbit resonance, the angle x is always oriented along the direction of r, which implies that the satellite always points the same face to the host planet. The Moon is presently trapped in a 1:1 spin-orbit resonance, while Mercury is observed to move in a 3:2 resonance.

B. The truncated conservative equation

Equation (1) can be written as

$$\ddot{x}+\varepsilon V_x(x,t)=0,$$

where $V(x,t)=-1/2(a/r)^3\cos(2x-2f)$ and V_x denotes the partial derivative. In view of Eq. (2) one can expand $V_x(x,t)$ in Fourier series as

$$\ddot{x}+\varepsilon\sum_{m\neq0,m=-\infty}^{\infty}W\left(\frac{m}{2},e\right)\sin(2x-mt)=0, \tag{3}$$

where the coefficients $W(m/2,e)$ decay as powers of the eccentricity, $W(m/2,e)=O(e^{|m-2|})$. To give an example we report the explicit expressions of some of these coefficients,

$$W\left(\frac{1}{2},e\right)=-\frac{e}{2}+\frac{e^3}{16}-\frac{5e^5}{384}+O(e^7),$$

$$W(1,e)=1-\frac{5e^2}{2}+\frac{13e^4}{16}-\frac{35e^6}{288}+O(e^8),$$

$$W\left(\frac{3}{2},e\right)=\frac{7e}{2}-\frac{123e^3}{16}+\frac{489e^5}{128}+O(e^7),$$

$$W(2,1)=\frac{17e^2}{2}-\frac{115e^4}{6}+\frac{601e^6}{48}+O(e^8).$$

For ease of computation it is sometimes convenient to consider a truncation of the series expansion appearing in Eq. (3). In particular we retain only those terms whose magnitude is bigger than the contribution of the neglected terms, like the tidal torque, external perturbations, etc. (we refer to Ref. 2 for a detailed discussion). For the Moon-Earth case we are led to consider the equation

$$\begin{aligned}\ddot{x}+\varepsilon\Bigg[&\left(-\frac{e}{2}+\frac{e^3}{16}\right)\sin(2x-t)+\left(1-\frac{5}{2}e^2+\frac{13}{16}e^4\right)\sin(2x-2t)\\&+\left(\frac{7}{2}e-\frac{123}{16}e^3\right)\sin(2x-3t)+\left(\frac{17}{2}e^2-\frac{115}{6}e^4\right)\\&\times\sin(2x-4t)+\left(\frac{845}{48}e^3-\frac{32525}{768}e^5\right)\sin(2x-5t)\\&+\frac{533}{16}e^4\sin(2x-6t)+\frac{228347}{3840}e^5\sin(2x-7t)\Bigg]=0.\end{aligned} \tag{4}$$

The case Mercury-Sun would deserve more components because the orbital eccentricity of Mercury is quite large. Nevertheless in the first instance we limit to consider Eq. (4) also for Mercury and we shall compare the results obtained by using Eq. (4) with those obtained using the complete Eq. (1).

C. The dissipative model

Different mathematical formulations are available in the literature to express the tidal torque acting on the satellite. Here we adopt the MacDonald expression which assumes a phase lag depending linearly on the angular velocity (see, e.g., Refs. 8, 7, 12, and 5). Let us write the dissipative equation as

$$\ddot{x}+\varepsilon\left(\frac{a}{r}\right)^3\sin(2x-2f)=T, \tag{5}$$

where T denotes the MacDonald tidal torque,[12]

$$T=-K\frac{a^6}{r^6}(\dot{x}-\dot{f}), \tag{6}$$

with K the dissipation constant, depending on the physical and orbital characteristics of the satellite. For the Moon and Mercury the value of K is about 10^{-8}. Taking the average of T over one orbital period, as is usual in this field (see, e.g., Ref. 5), one obtains

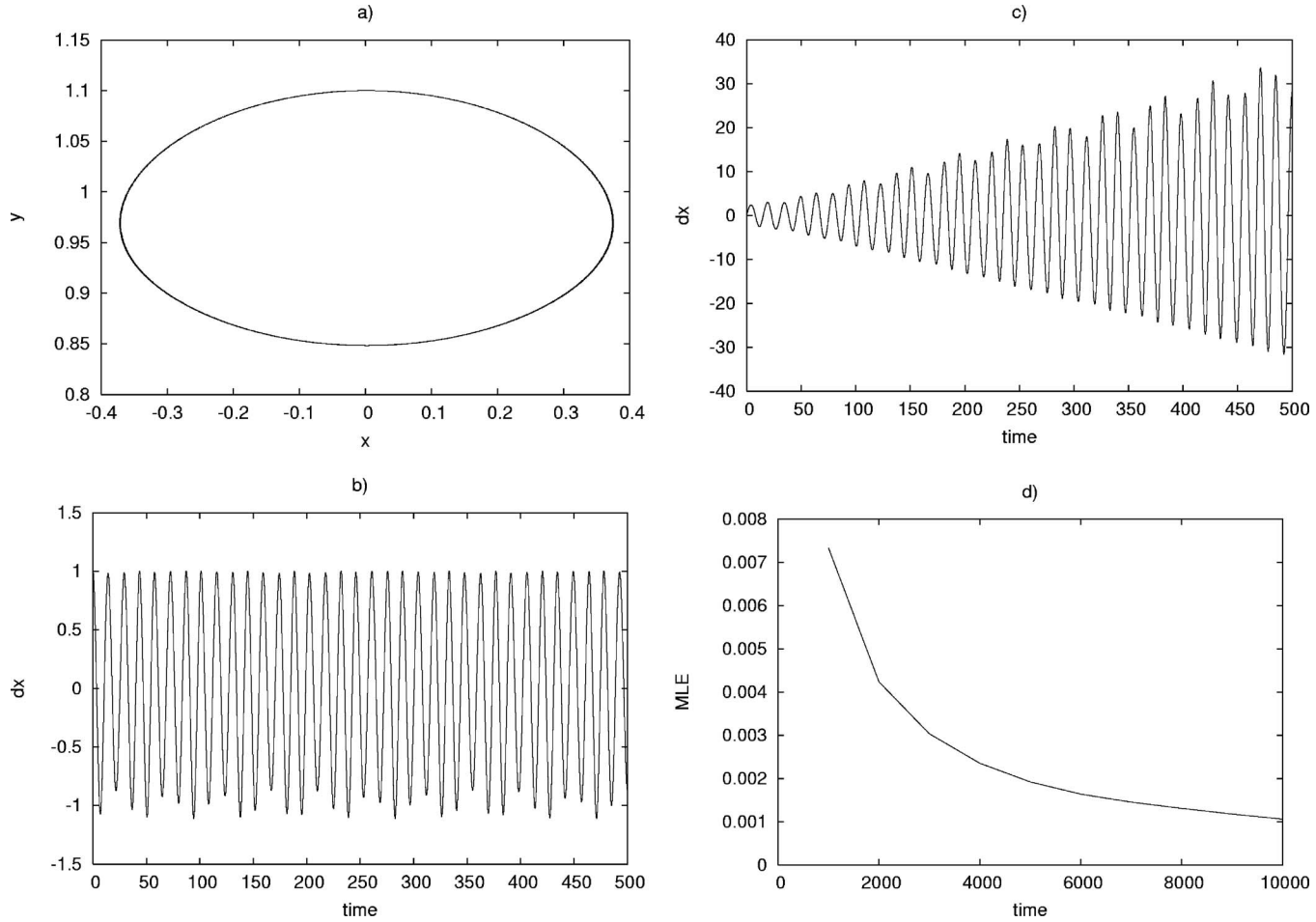

FIG. 1. An example of a librational invariant torus associated with Eq. (4) with $\varepsilon=0.1$, $e=0.0549$; the initial conditions are set to $x=0$, $y=1.1$. (a) Poincaré section on the plane $t=0$. (b) Conjugate points method starting with the horizontal tangent vector. (c) Conjugate points method starting with the vertical tangent vector. (d) Finite-time maximum Lyapunov exponent (MLE).

$$\langle T\rangle = -K[L(e)\dot{x} - N(e)]$$

with

$$L(e) \equiv \frac{1}{(1-e^2)^{9/2}}\left(1+3e^2+\frac{3}{8}e^4\right),$$

$$N(e) \equiv \frac{1}{(1-e^2)^{6}}\left(1+\frac{15}{2}e^2+\frac{45}{8}e^4+\frac{5}{16}e^6\right).$$

Taking into account the dissipative contribution, the equation of motion becomes

$$\ddot{x} + \varepsilon\left(\frac{a}{r}\right)^3 \sin(2x-2f) = K[N(e) - L(e)\dot{x}]. \tag{7}$$

III. NONEXISTENCE OF ROTATIONAL INVARIANT TORI

We investigate the models (1) and (4)–(7); since r, f are periodic functions of time, such models are defined for $(x,y,t) \in \mathbf{T}\times\mathbf{R}\times\mathbf{T}$, with $y=\dot{x}$. In particular we will be concerned with the nonexistence of rotational invariant tori. The key hypothesis on which the methods depend is *twist*, which in the present context can be taken to mean (this condition implies that the first return map is a composition of twist maps and therefore is a tilt map, which is a sufficient hypothesis for the application of the nonexistence criterion)

$$\frac{\partial \dot{x}}{\partial y} \geqslant C > 0$$

for some constant C. Of course this is satisfied for the spin-orbit models (with $C=1$).

In this section we present numerical results, while some analytical estimates are given in Appendix A. For the purposes of the present paper, a *rotational* torus is the graph

$$y = v(x,t), \quad (x,t) \in \mathbf{T}^2,$$

of some continuous function v. Figure 4 will show an example of a rotational invariant torus in a Poincaré section.

Rotational tori are to be contrasted with other possible types of torus. For example, there can be invariant tori of the form $r=R(\theta,t)$ in polar coordinates (r,θ) about a periodic orbit of period 2π (e.g., Fig. 1). There can be invariant tori which form chains of islands in a Poincaré section around a p/q-resonant periodic orbit of period $2\pi q$, $q>1$ (not shown), and there can be invariant tori which form chains of islands around periodic orbits whose period is a multiple of the order of resonance, as in Fig. 2. We lump all these under

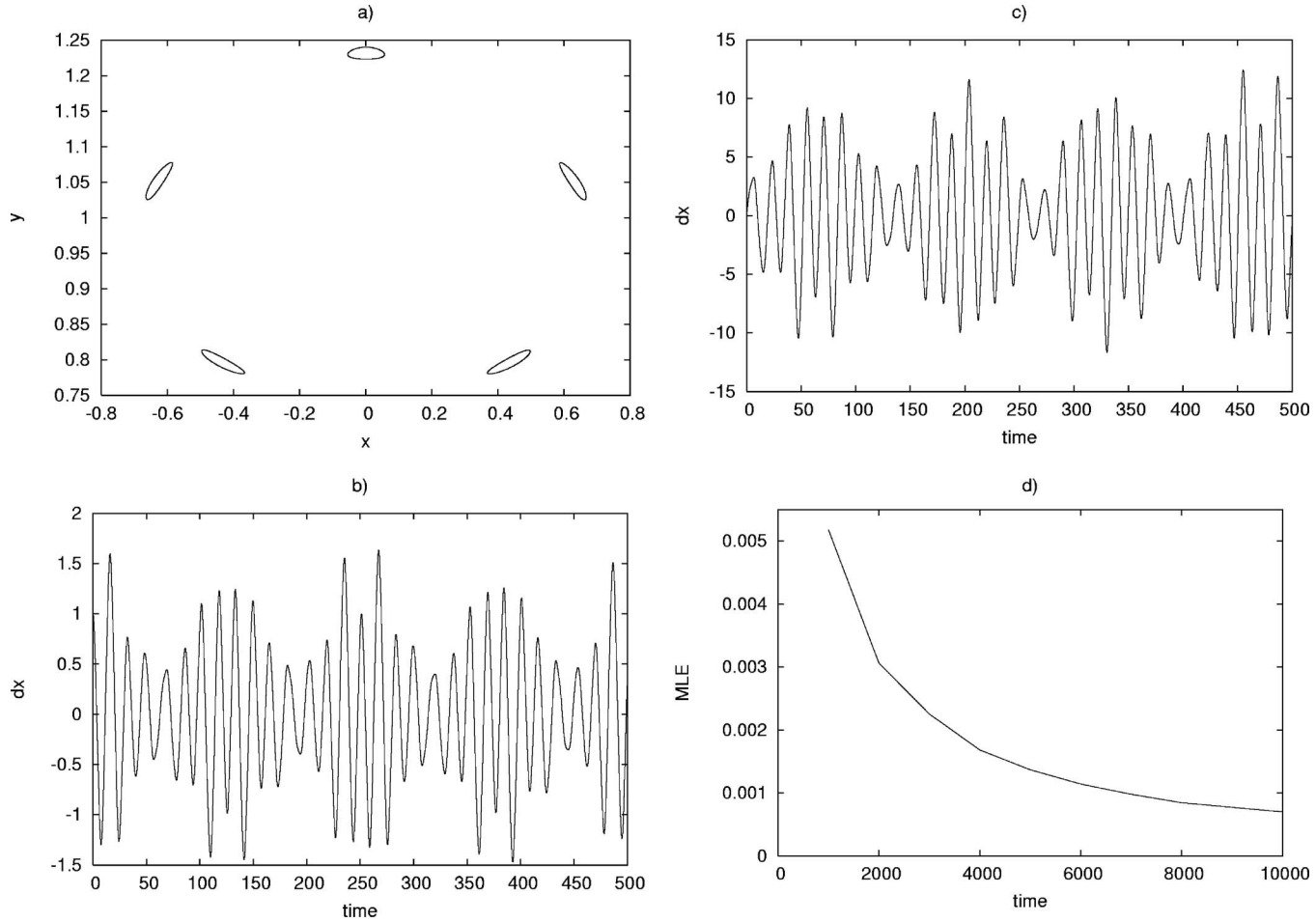

FIG. 2. An example with a chain of islands associated with Eq. (4) with $\varepsilon=0.1$, $e=0.0549$; the initial conditions are set to $x=0$, $y=1.24$. (a) Poincaré section on the plane $t=0$. (b) Conjugate points method starting with the horizontal tangent vector. (c) Conjugate points method starting with the vertical tangent vector. (d) Finite-time maximum Lyapunov exponent (MLE).

the term *librational* invariant tori, although some authors might reserve the term for just the first type.

A torus that is not a graph but is continuously deformable to a graph could also be counted as rotational. In the conservative case, however, a theorem of Birkhoff[1] ensures that such cases do not occur as invariant tori, because of twist. In the dissipative case, the theorem does not apply, and indeed invariant tori which are continuously deformable to graphs but not graphs can occur; we exclude them from the definition of rotational because the criterion we will use applies only to graphs.

A. The conjugate points criterion

The numerical analysis of the nonexistence of invariant tori is based on the conjugate points criterion.[9] It was developed in the context of conservative dynamics, but suitably interpreted it applies to dissipative systems too. Below we sketch the content of the method in a form which applies to both conservative and dissipative systems.

Conjugate points criterion: Let (x,y): $[t_0,t_1]\to \mathbf{T}\times\mathbf{R}$ be an orbit; the times t_0 and t_1 are said to be *conjugate* for the orbit, if there is a nonzero tangent orbit $(\delta x,\delta y)$ such that $\delta x(t_0)=\delta x(t_1)=0$. The existence of conjugate points implies that (x,y) does not belong to any rotational invariant torus, or else the forward orbit of an initial *vertical* vector $(0,1)$ at $t=t_0$ is prevented from crossing the tangent to the torus and so twist obliges it to have $\delta x(t)>0$ for all $t>t_0$.

For a system with time-reversal symmetry under $(x,y)\to(-x,y)$ [as in the conservative case Eq. (1) if the origin of time is taken to have $f=0$] and initial conditions on the symmetry line $x=0$, one can obtain the backward trajectory and the backward tangent orbit by reflecting the forward ones. So times $\pm t$ are conjugate if the tangent orbit of the *horizontal* vector $(\delta x,\delta y)(0)=(1,0)$ has $\delta x(t)=0$. This observation can more than halve the time required to obtain conjugate points, because not only do we obtain orbits of twice the length but also if the symmetry line is well chosen (dominant, see, e.g., Ref. 9) the rotation of tangent orbits is strongest near there, so it is best to choose orbit segments which straddle it symmetrically.

Without such a symmetry (as in the dissipative case), one has to integrate backwards and forwards independently. The lengths of backwards and forwards times can be chosen independently, however, so one can choose just to take $t_0=0$ and do no backward integration. This means we integrate forwards from the vertical vector $(\delta x,\delta y)(0)=(0,1)$ and look for a sign change in $\delta x(t)$. Alternatively one could integrate in both directions of time from a horizontal tangent vector

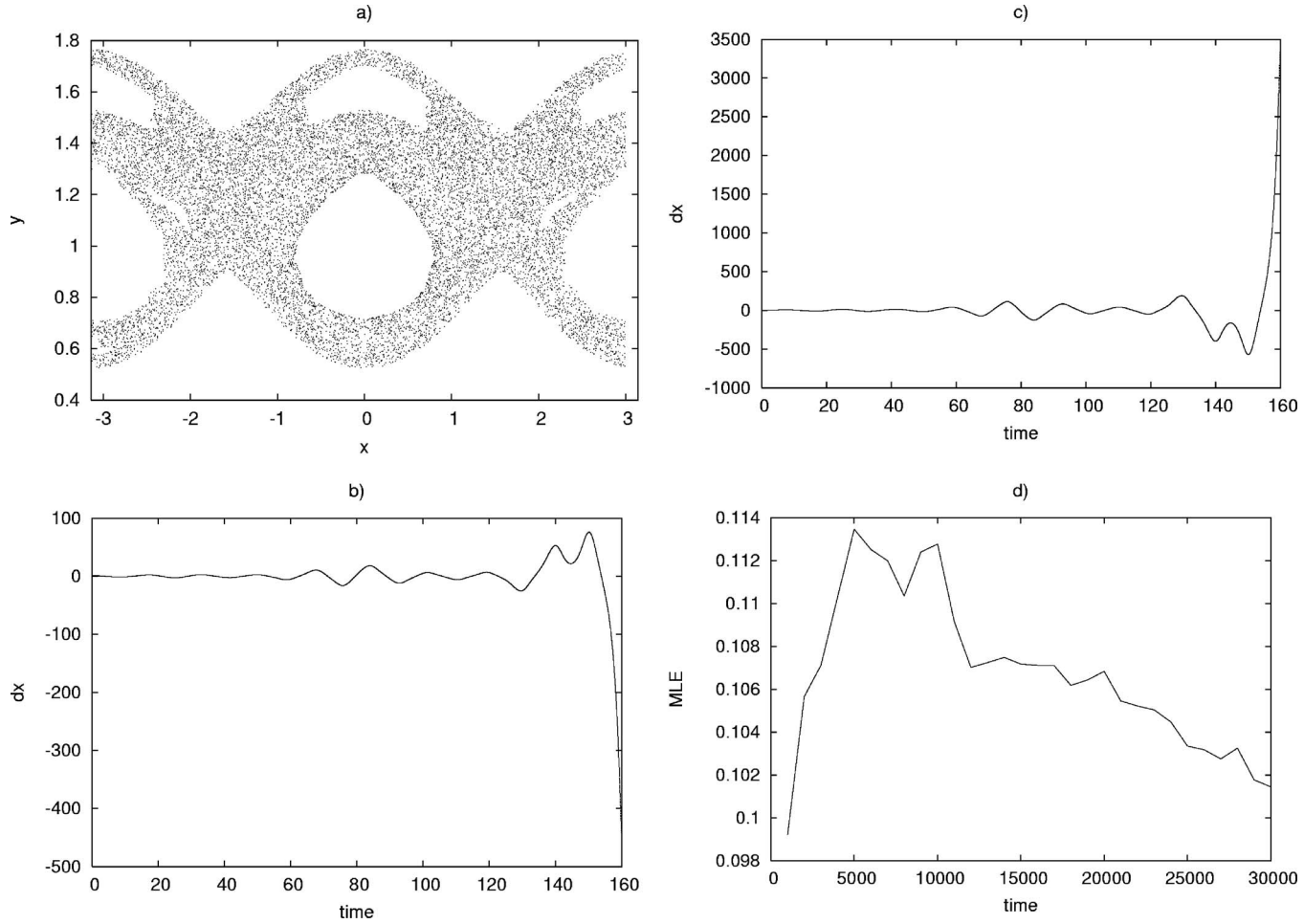

FIG. 3. An example of chaotic motion associated with Eq. (4) with $\varepsilon=0.1$, $e=0.0549$; the initial conditions are set to $x=0$, $y=1.3$. (a) Poincaré section on the plane $t=0$. (b) Conjugate points method starting with the horizontal tangent vector. (c) Conjugate points method starting with the vertical tangent vector. (d) Finite-time maximum Lyapunov exponent (MLE).

(or any vector with $\delta x>0$) and look for $t_0<0$ and $t_1>0$ such that $\delta x(t_1)=\delta x(t_2)=0$. A slightly more sophisticated way to handle this case is the cone-crossing criterion, described in Appendix B.

B. Tangent orbit indicator

We now give some examples to verify the nonexistence criterion by looking for sign changes in $\delta x(t)$. The numerics reveal that one can learn more from $\delta x(t)$ if it does change sign, distinguishing between rotational tori, librational tori, and chaos, leading us to introduce a "tangent orbit indicator."

In case of a librational curve with horizontal initial tangent vector, the δx-component shows oscillations around zero; the amplitude increases linearly when starting from the vertical tangent vector. We report an example in Fig. 1 obtained by integrating Eq. (4) through a fourth-order symplectic Yoshida's method;[14] it is enough to integrate up to $t=500$ to recognize the librational character of the motion due to the successive oscillations around zero. If one just wants to establish the nonexistence of rotational invariant tori, it is sufficient to determine the first crossing, which occurs almost immediately at $t=3.39$. A similar result is obtained for the chain of islands shown in Fig. 2, where the first crossing occurs at $t=3.51$. In both cases the maximum Lyapunov exponent (hereafter, MLE) seems to converge to zero, while it does not converge for chaotic motions as shown in Fig. 3 where the nonexistence criterion provides severe oscillations of very large amplitudes with the first crossing of the zero line at $t=3.64$. As far as rotational invariant tori (Fig. 4) are concerned, the nonexistence method correctly does not show changes in sign of δx, but rather positive oscillations of increasing amplitude. The corresponding MLE converges to zero.

We remark that the interval of time necessary to obtain reliable results is definitely longer for the Lyapunov exponents than for the nonexistence criterion (compare the time scales in Figs. 1–4). Indeed, after the first change of sign of δx we can already exclude the existence of rotational invariant tori through the given point.

Moreover, in contrast to the Lyapunov exponents, the nonexistence criterion allows us to distinguish between chaotic motions, librational tori, and rotational tori, extending the idea of the fast Lyapunov indicators.[6,15] In order to have a global view of the dynamics, we introduce a quantity based on the conjugate points criterion, which we call a *tangent orbit indicator*. More precisely, we compute the average over a finite interval of time (say $t=100$) of $\delta x(t)$. According to the value of this quantity one can discern the behavior of the

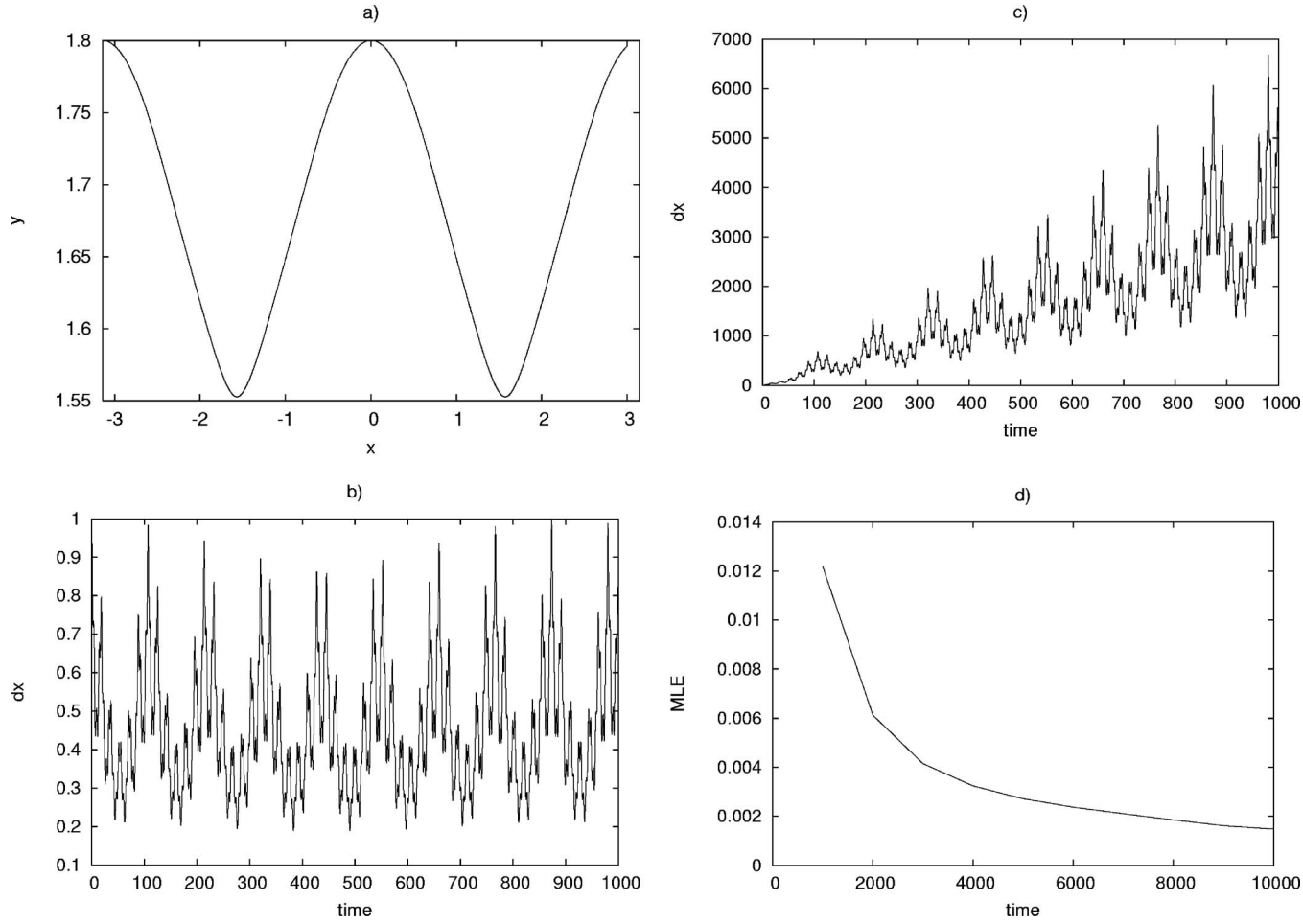

FIG. 4. An example of a rotational invariant torus associated with Eq. (4) with $\varepsilon=0.1$, $e=0.0549$; the initial conditions are set to $x=0$, $y=1.8$. (a) Poincaré section on the plane $t=0$. (b) Conjugate points method starting with the horizontal tangent vector. (c) Conjugate points method starting with the vertical tangent vector. (d) Finite-time maximum Lyapunov exponent (MLE).

dynamics: zero value denotes a librational regime, a moderate value is associated to rotational tori, while high values correspond to chaotic motions. It is useful to visualize such results by assigning a color as follows:

- black or blue for tangent orbit indicators close to zero;
- red to orange for moderate values;
- yellow for large values of the tangent orbit indicator.

As an example we report in Fig. 5 (top panels) the computation of the tangent orbit indicators over a grid of 500 $\times$500 initial conditions with $x\in[0,2\pi]$ and $y\in[0.5,2.5]$ for Eq. (4), with horizontal initial tangent vector. Similarly one can proceed to explore the space of parameters by plotting the tangent orbit indicator, for example, in the plane y-ε for a fixed x_0. The results shown in Fig. 5 (bottom panels) are validated by the computation of the frequency analysis, obtained by evaluating the frequency of motion versus the initial condition $y(0)$ (see Fig. 6).

We conclude this subsection with proofs that the generic behavior of $\delta x(t)$ for an orbit on an invariant torus in the conservative case with vertical initial vector is quasiperiodic oscillation with linear growth, between two lines with positive slope in the rotational case, or with opposite signs and mean zero in the librational case, and for the case of systems with time-reversal symmetry, symmetric initial condition and horizontal initial tangent vector, the generic behavior on an invariant torus is bounded quasiperiodic oscillation, with no zeros if rotational, mean zero if librational.

For a rotational invariant torus, generically there is a coordinate system (X,Y) [depending on (x,y,t)] in which the torus is $Y=0$ and the linearized motion $\delta Y(t)$ is constant, $\delta X(t)=\delta X(0)+\tau\delta Y(0)$, for some τ called the normal torsion of the torus. Because of twist, $\tau>0$. Thus in this coordinate system $\delta X(t)$ grows exactly linearly with t. Transforming back to the original coordinates, we have $\delta x(t)=\partial x/\partial X\delta X(0)+(\partial x/\partial X\tau+\partial x/\partial Y)\delta Y(0)$. The partial derivatives are generically quasiperiodic functions of t, so if $\delta Y(0)>0$, as for vertical initial vector, one obtains oscillation between two lines of linear growth. Both lines have positive slope, or else $\delta x(t)$ would become negative at some time, which is forbidden. If $\delta Y(0)=0$, as in the symmetric case with horizontal initial vector, then only the first term contributes and $\delta x(t)$ performs bounded quasiperiodic oscillations (by symmetry the torus crosses the symmetry line horizontally, so the tangent orbit remains tangent to the invariant torus).

For a librational torus, the tangent to the torus makes one full revolution for each revolution of the base point around

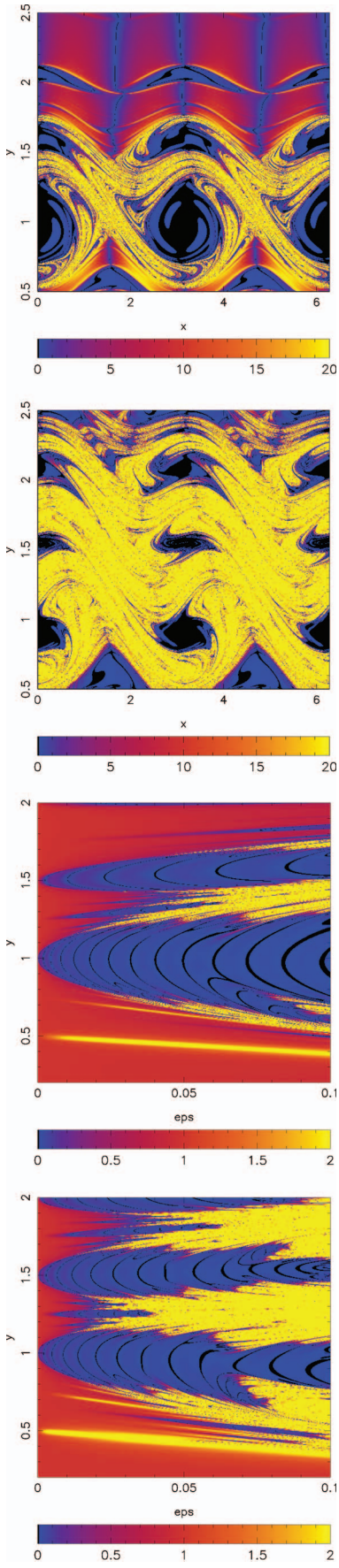

FIG. 5. (Color) Tangent orbit indicator associated with Eq. (4) for $\varepsilon=0.1$ starting from the horizontal tangent vector. From top to bottom: graph in the plane x-y with $e=0.0549$; graph in the plane x-y with $e=0.2056$; graph in the plane ε-y with $e=0.0549$; graph in the plane ε-y with $e=0.2056$.

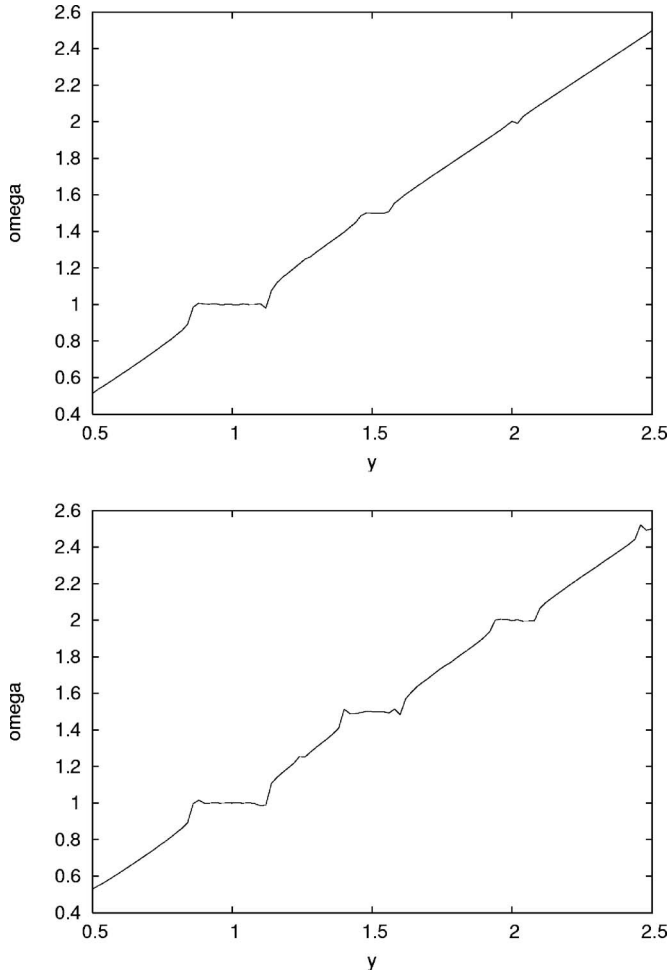

FIG. 6. Computation of the frequency ω associated with Eq. (4) vs the initial condition y for $\varepsilon=0.01$ and $x(0)=0$; top: $e=0.0549$; bottom: $e=0.2056$.

the torus. The tangent orbit of the initial vertical vector is obliged to remain on the same side of the tangent all the time, thus it has to keep turning. This obliges its x-component to oscillate with mean zero. Generically the torsion of a librational torus is nonzero, hence the oscillations grow linearly. In the symmetric case with horizontal initial vector, it is tangent to the torus so its orbit performs quasiperiodic oscillations with zero mean because averaging the tangent vector over the torus must make a full turn back to the starting point.

C. The conservative models

Now we consider the complete and truncated spin-orbit models provided by Eqs. (1) and (4) and make a detailed scan of parameter and phase space. The integration of such systems is performed by Yoshida's symplectic method[14] with step-size $h=10^{-2}$ and conjugate points are computed up to $t_{\max}=150$; a grid of 500×500 points over the initial velocity $y\equiv\dot{x}$ and ε has been investigated. The other initial conditions have been set to $x_0=0$, $\delta x=1$, $\delta\dot{x}=0$ [making use of time-reversal symmetry, we are looking for $x(\pm t)$ to be conjugate]. Two cases have been considered: $e=0.0549$ (i.e., Moon's eccentricity) and $e=0.2056$ (i.e., Mercury's eccentricity). Fig-

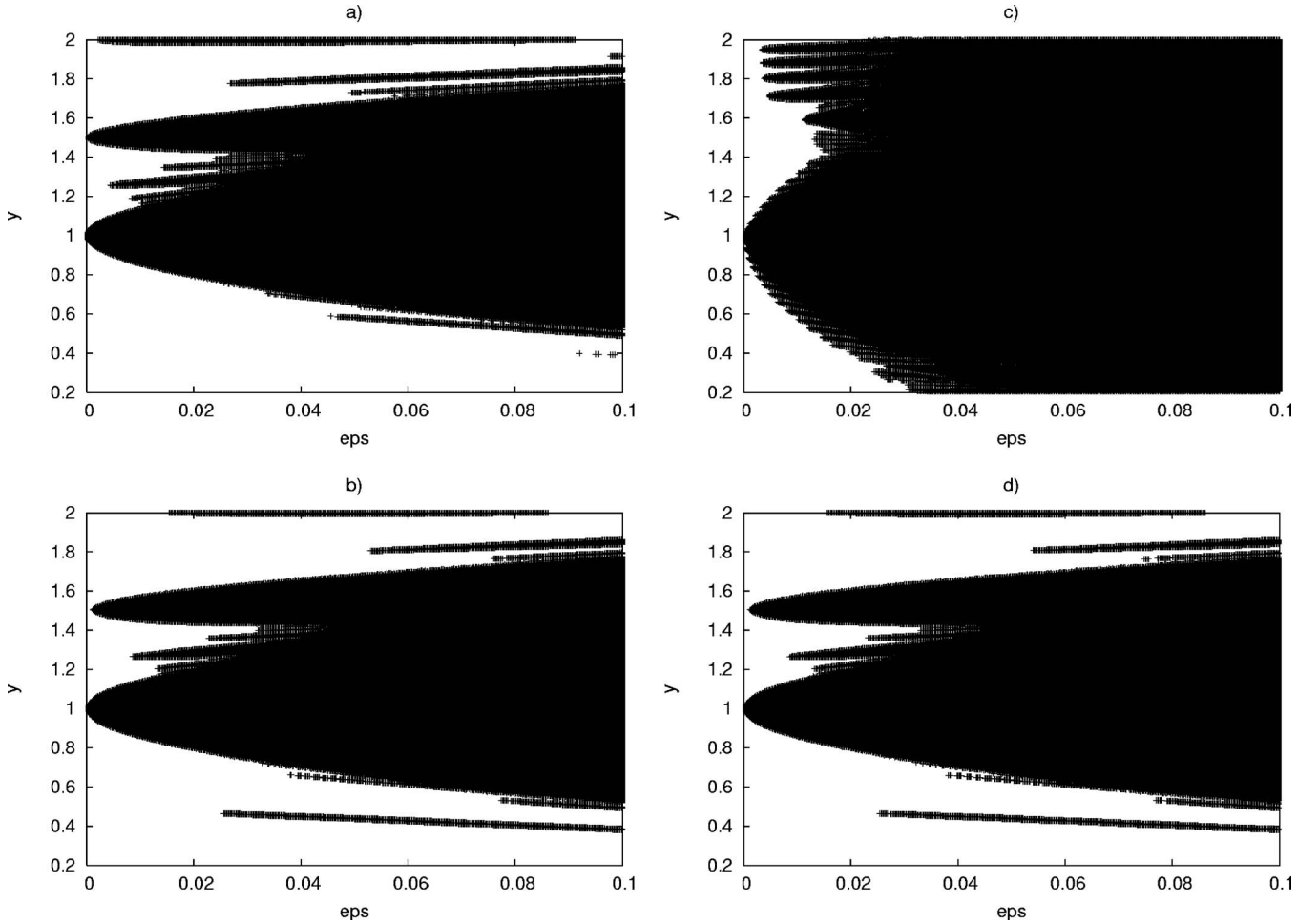

FIG. 7. The black region denotes the nonexistence of rotational invariant tori for $e=0.0549$ associated with (a) Eq. (1) starting from the horizontal tangent vector; (b) Eq. (7) with $K=10^{-4}$ starting from the vertical tangent vector; (c) Eq. (7) with $K=10^{-2}$ starting from the vertical tangent vector; (d) Eqs. (5) and (6) with $K=10^{-4}$ starting from the vertical tangent vector.

ures 7(a) and 8(a) locate a zone (black region) where invariant rotational tori associated with Eq. (1) are deduced not to exist and therefore they also provide an estimate of the amplitude of the librational region around a given resonance. (A $p:q$ resonance corresponds to $y=p/q$ at $\varepsilon=0$.) The white region can be tori or not; in the limit of infinite computation and if we examined every vertical, not just the dominant symmetry line, the white region is filled by tori.[13] Indeed for the Moon the 1:1 resonance has a librational extent larger than the 3:2 resonance [Fig. 7(a)], while for Mercury the two resonances appear to have about the same amplitude [Fig. 8(a)].

We have performed the same computations for the truncated Eq. (4), selecting the same values of parameters and initial conditions. The results show a qualitatively similar behavior, thus indicating the validity of the truncated model, both for the Moon and Mercury's eccentricity, as far as nonexistence of rotational invariant tori is concerned.

D. The dissipative models

We applied the same criterion for nonexistence of rotational invariant tori to the dissipative models (5)–(7), but starting from $\delta x=0$, $\delta\dot{x}=1$, as the dissipative system does not have time-reversal symmetry. The method was applied up to $t_{\max}=150$ over a grid of 500×500 points in the plane ε-y, integrating the equation of motion by Yoshida's method with step-size $h=10^{-2}$. We remark that although we call the method symplectic, it is not in general symplectic when applied to a non-Hamiltonian vector-field.

Different values of the dissipation factor were used, namely, $K=10^{-4}$ [Figs. 7(b) and 8(b)], $K=10^{-2}$ [Figs. 7(c) and 8(c)]. The region where the method gives nonexistence gets wider as the dissipation increases (compare with Ref. 4). Very similar results are obtained using the model Eqs. (5) and (6) with time-dependent dissipation [Figs. 7(d) and 8(d)]; indeed the graphs obtained using Eqs. (7), (5), and (6) can be essentially superimposed, thus indicating that for the present values of the parameters it suffices to consider the averaged model described by Eq. (7). As in the conservative case, for higher eccentricities the extent of the 3:2 resonance increases with respect to the synchronous one.

Some words are required about the interpretation of the results in the dissipative case. Unlike the conservative case, it is not correct to assume that if the method is run for long enough then every initial condition that is not excluded by the method lies on a rotational invariant torus. All points in a

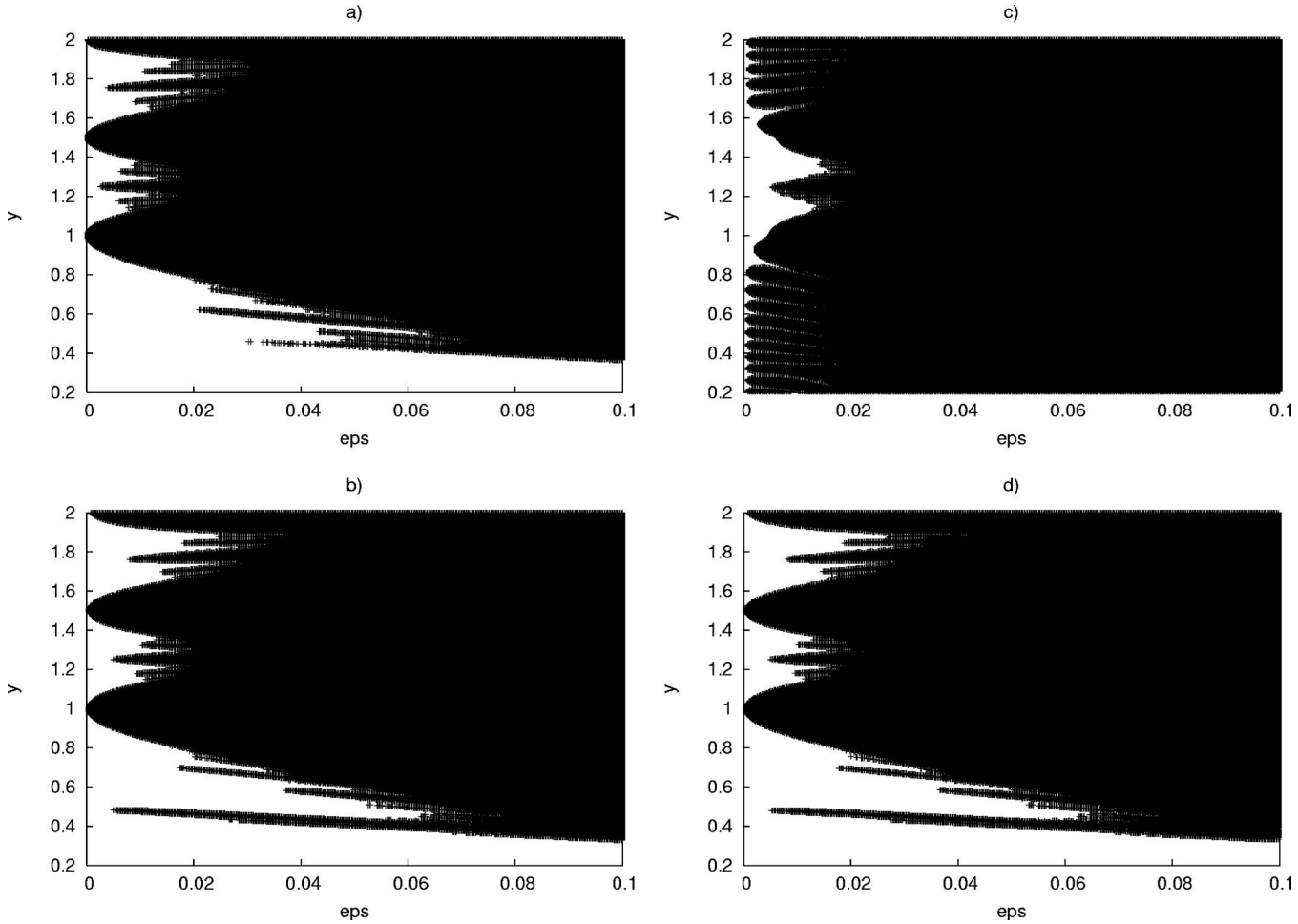

FIG. 8. The black region denotes the nonexistence of rotational invariant tori for $e=0.2056$ associated with (a) Eq. (1) starting from the horizontal tangent vector; (b) Eq. (7) with $K=10^{-4}$ starting from the vertical tangent vector; (c) Eq. (7) with $K=10^{-2}$ starting from the vertical tangent vector; (d) Eqs. (5) and (6) with $K=10^{-4}$ starting from the vertical tangent vector.

sufficiently small neighborhood of attraction of a rotational invariant torus also have forward orbits with no conjugate points. Thus the regions of nonexistence given by our criterion avoid a neighborhood of each attracting rotational invariant torus.

Also, one should not expect many points to lie on a rotational invariant torus. For models like Eqs. (6) and (7), where the dissipation leads to contraction of area everywhere [at rate Ka^6/r^6 for Eq. (6) and KL for Eq. (7)], there can be at most one rotational invariant torus, or else the region in between two of them would be simultaneously invariant and contracted. Even if the dissipation does not have a constant sign, generically, a rotational invariant torus of a dissipative system is isolated, because attracting (or repelling), so we do not expect many initial conditions to lie on rotational invariant tori.

In addition, in a dissipative system there can be invariant tori continuously deformable to rotational tori, but not rotational. For example, take the damped pendulum

$$\dot{x}=y, \quad \dot{y}=\sin x-\nu y$$

(independent of t, so trivially of period 2π in t) with subcritical damping $\nu\in(0,2)$. It has an invariant circle (hence torus when extended in t) connecting the two equilibria (0,0) and $(\pi,0)$ (periodic orbits when extended in t) and separating large positive y from large negative y, but for $\nu\in(0,2)$ the eigenvalues at (0,0) are complex conjugate, so the invariant circle rolls up in a pair of infinite spirals around it. For any initial condition on this torus [apart from $(\pi,0)$], our method will declare after enough time that it is not on a rotational invariant torus, because of the roll-up. Probably the real Moon and Mercury are on such an invariant torus (to the extent that the models here apply). This is what Figs. 8(b) and 8(c) suggest: the regions of libration around $x=0,\pi$ are subject to slow area-contraction so one would see attracting spirals if resolved sufficiently.

E. Poincaré sections

The results shown in the previous sections are validated by the computation of the corresponding Poincaré sections in the plane (x,y) for the conservative case and for the dissipative samples (see Fig. 9). Passing from the conservative case [Fig. 9(a)] to the weakly dissipative regime with $K=10^{-6}$ [Fig. 9(b)], the main resonances are preserved, though the higher order ones are destroyed. For larger dissipation, say $K=10^{-4}$ [Fig. 9(c)], most of the orbits are attracted by the 1:1 and 3:2 periodic orbits, while for stronger dissipation, say

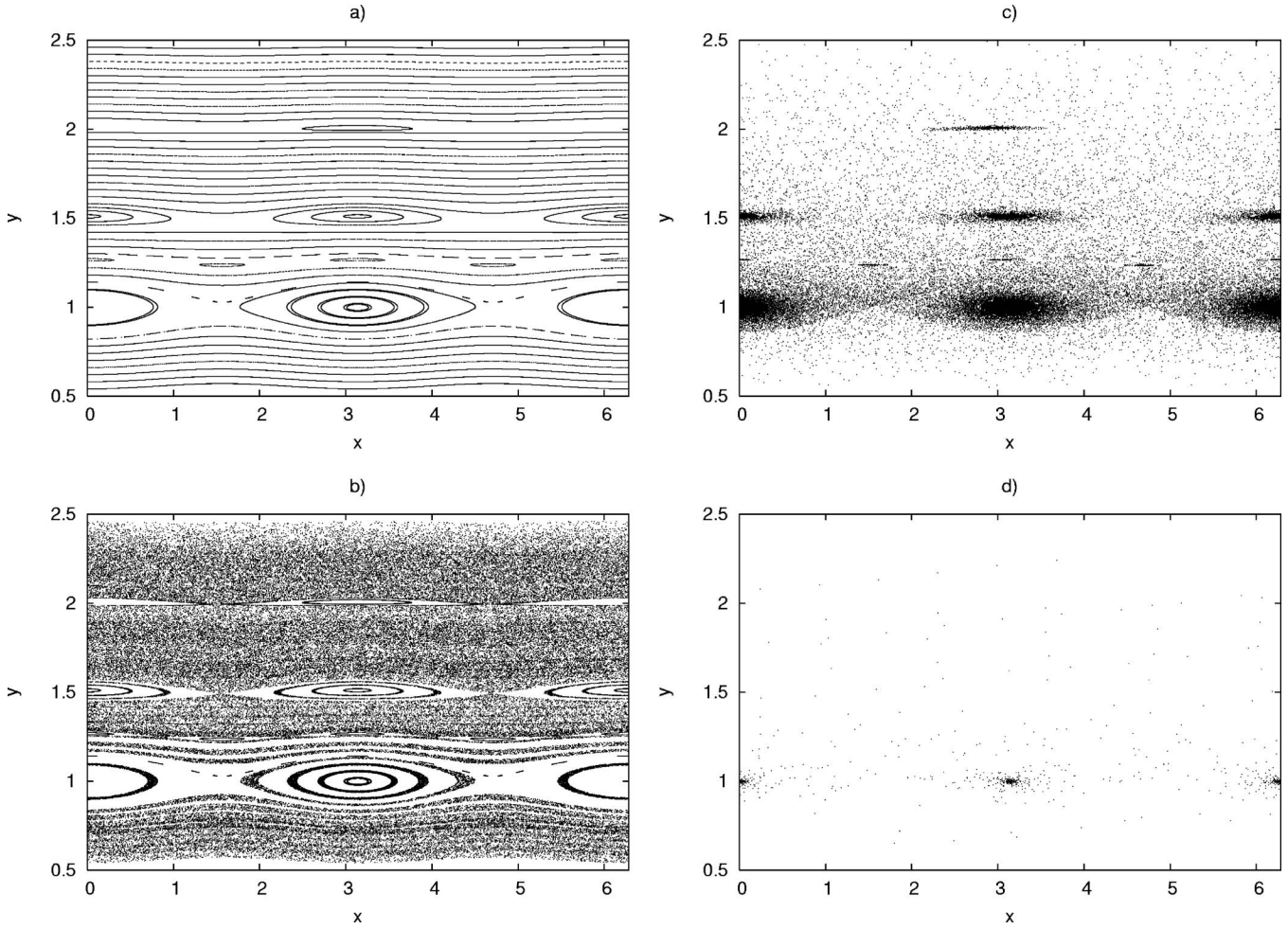

FIG. 9. Poincaré maps associated with Eq. (7) for $e=0.0549$ and $\varepsilon=0.01$. (a) $K=0$, (b) $K=10^{-6}$, (c) $K=10^{-4}$, (d) $K=10^{-2}$.

$K=10^{-2}$, the synchronous resonance dominates the whole region as shown in Fig. 9(d), being the only attractor in the considered domain.

The results provided in the dissipative context depend strongly on the overall computational time of conjugate points, which has been typically set to $t_{\max}=150$. But the conclusions might strengthen drastically as the time increases. To provide an example, we compare the results on the region where nonexistence associated with Eq. (7) is established over two different times, i.e., $t_{\max}=150$ and $t_{\max}=1500$ (see Fig. 10). Indeed we conclude by noticing that nonexistence of rotational invariant tori is established for a slightly larger region of (ε,y) space (see Fig. 10, where the results are computed over a grid of 150×150 points).

IV. CONCLUSIONS

The spin-orbit model has been investigated as a testbench of a numerical method aimed to determine the nonexistence of rotational invariant tori. In particular the *conjugate points* criterion has been widely exploited to study the dynamics. Indeed such method can be successfully used to discern between librational, rotational or chaotic motions. A comparison with standard methods, like the Lyapunov exponents or frequency analysis, has been also performed. There are several advantages when using the conjugate points technique: it has a strong background based on the analytical theory describing the converse KAM technique, it is very simple to implement and it runs relatively fast. The extension of such method to more general systems would be certainly of interest and could be used as a complementary tool to standard techniques.

APPENDIX A: ANALYTICAL ESTIMATES FOR THE TRUNCATED CONSERVATIVE MODEL

Let us write Eq. (4) as

$$\ddot{x}+\varepsilon\sum_{m=1}^{7}\alpha_m(e)\sin(2x-mt)=0 \tag{A1}$$

with the obvious identification of the coefficients $\alpha_m(e)$ which turn out to be a truncation of the coefficients $W(m/2,e)$ [for example, $\alpha_2(e)=1-5/2e^2+13/16e^4$]. We apply the nonexistence criterion for rotational invariant tori developed in Ref. 9 on the basis of Weierstrass' theorem. The result applies in arbitrarily many degrees of freedom, but we specialize it here to the present case. Consider a Lagrangian $L(x,\dot{x},t)$ on $\mathbf{T}\times\mathbf{R}\times\mathbf{T}$ with the second derivative $L_{\dot{x}\dot{x}}>0$ and let $x:\mathbf{R}\to\mathbf{T}$ be a trajectory; let W be the action associated to the Lagrangian L.

Criterion: If $x:[t_0,t_1]\to\mathbf{T}$ is not a nondegenerate mini-

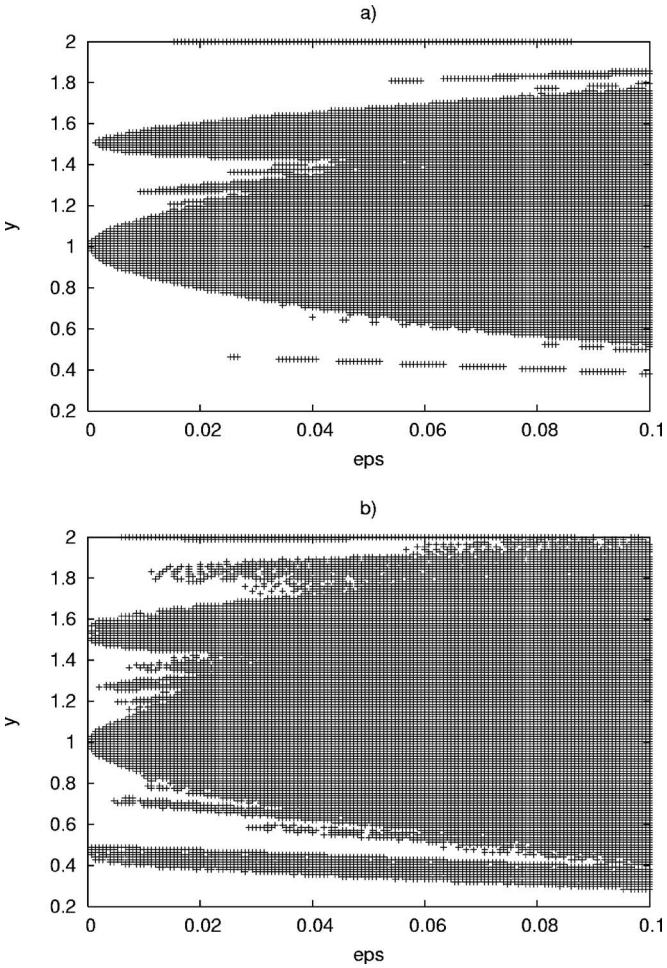

FIG. 10. Nonexistence of invariant rotational tori associated with Eq. (7) for $e=0.0549$ and $K=10^{-4}$ starting from the vertical tangent vector. (a) $t_{\max}=150$, (b) $t_{\max}=1500$.

mum of the action W associated with L, then x is not contained in any rotational invariant graph.

The practical implementation of such criterion requires to evaluate when the second variation of the action fails to be positive definite for $\delta x(t_i)$ vanishing at the ends.

We proceed to apply this criterion to Eq. (A1), whose associated Lagrangian function takes the form

$$L(x,\dot{x},t)=\frac{1}{2}\dot{x}^2+\frac{\varepsilon}{2}\sum_{m=1}^{7}\alpha_m(e)\cos(2x-mt),$$

while the second variation of the action is

$$\delta^2 W=\int_{t_0}^{t_1}\left[\delta\dot{x}^2-2\varepsilon\sum_{m=1}^{7}\alpha_m(e)\cos(2x-mt)\,\delta x^2\right]dt.$$

Let us consider the deviation $\delta x(t)=\cos t/4\tau$ such that $\delta x(\pm 2\pi\tau)=0$; for later use we notice that $\int_0^{2\pi\tau}\delta x^2=\pi\tau$, $\int_0^{2\pi\tau}\delta\dot{x}^2=\pi/16\tau$. Let us write Eq. (A1) as

$$\ddot{x}=f(x,t)\equiv-\varepsilon\sum_{m=1}^{7}\alpha_m(e)\sin(2x-mt);$$

assuming the initial conditions $x(0)=0$, $\dot{x}(0)=v_0$ we note that the solution of Eq. (A1) is odd and we write the solution in the integral form as

$$x(t)=v_0 t+\int_0^t (t-s)f(x(s),s)ds.$$

Let H be an upper bound for $f(x,t)$, i.e., $|f(x,t)|\leqslant\varepsilon\Sigma_{m=1}^{7}|\alpha_m(e)|\equiv H$; as a first approximation we can use

$$|x(t)-v_0 t|\leqslant\frac{H}{2}t^2.$$

Using the estimate $\cos\theta\geqslant 1-1/2\theta^2$, we get

$$\cos(2x-mt)\geqslant 1-\tfrac{1}{2}(|m-2v_0|t+Ht^2)^2.$$

Therefore we obtain that the second variation of the action for the variation $\delta x(t)=\cos t/4\tau$, $-2\pi\tau\leqslant t\leqslant 2\pi\tau$, is bounded by

$$\begin{aligned}\delta^2 W&\leqslant\frac{\pi}{8\tau}-4\varepsilon\sum_{m=1}^{7}|\alpha_m(e)|\\&\quad\times\int_0^{2\pi\tau}\left[1-\frac{1}{2}(|m-2v_0|t+Ht^2)^2\right]\delta x^2 dt\\&\leqslant\frac{\pi}{8\tau}-4H\pi\tau+2\varepsilon\sum_{m=1}^{7}|\alpha_m(e)|\\&\quad\times\int_0^{\pi/2}[|m-2v_0|^2(4\tau)^3\theta^2\\&\quad\times\cos^2\theta+H^2(4\tau)^5\theta^4\cos^2\theta\\&\quad+2|m-2v_0|H(4\tau)^4\theta^3\cos^2\theta]d\theta.\end{aligned}$$

Setting

$$I_n\equiv 2\int_0^{\pi/2}\theta^n\cos^2\theta\,d\theta,$$

one finds

$$\begin{aligned}\frac{\delta^2 W}{\tau}&\leqslant\frac{\pi}{8\tau^2}-4H\pi+\frac{\varepsilon}{\tau}\sum_{m=1}^{7}|\alpha_m(e)|\cdot[|m-2v_0|^2(4\tau)^3 I_2\\&\quad+2|m-2v_0|H(4\tau)^4 I_3+H^2(4\tau)^5 I_4]\equiv\Phi(\varepsilon,v_0,\tau).\end{aligned}\tag{A2}$$

The nonexistence criterion relies on the study of the sign of the function $\Phi(\varepsilon,v_0,\tau)$; nonexistence is guaranteed whenever one can find $\tau>0$ such that $\Phi(\varepsilon,v_0,\tau)$ is negative, implying that $\delta^2 W<0$. Let us denote by ε_{NE} the value of the perturbing parameter at which this condition first occurs.

We consider the two special cases provided by $e=0.0549$ and $e=0.2056$; such values of the eccentricity correspond to the Moon and Mercury, respectively. Moreover, we take into account two values of v_0, i.e., $v_0=1$ and $v_0=1.5$, which correspond, respectively, to the 1:1 and to the 3:2 resonance. The results of the implementation of the

TABLE I. Results based on Eq. (A2).

	Moon	Mercury
$v_0=1$	$\varepsilon_{NE}\simeq 0.15$	$\varepsilon_{NE}\simeq 0.82$
$v_0=1.5$	$\varepsilon_{NE}\simeq 0.77$	$\varepsilon_{NE}\simeq 0.58$

above criterion based on the estimate (A2) are summarized in Table I. It provides values much larger than the actual values of the oblateness, whereas the previous numerics indicates nonexistence in tongues around these low order rational initial velocities right down to $\varepsilon=0$ for the conservative dynamics [Figs. 7(a) and 8(a)] [and even for the weakly dissipative cases, Figs. 7(b), 7(c), 8(b), and 8(c)]. This failure is not surprising, however, since the estimates of this appendix are crude. The point of the appendix is only to show that some explicit regions of nonexistence of rotational invariant tori can be found by hand.

APPENDIX B: CONE-CROSSING CRITERION

Without assuming time-reversal symmetry under $(x,y)\to(-x,y)$ or initial conditions on a symmetry line, one could apply the conjugate points criterion with $t_0=-t_1$ if one could guess the slope of an initial tangent vector $(\delta x,\delta y)(0)$ such that $\delta x(\pm t_1)=0$ simultaneously. This can be achieved by computing monodromy matrices $M(\pm t)$ governing how the orbits of arbitrary initial tangent vectors evolve,

$$\dot{M}=F_{\underline{z}}M,$$

with $M(0)=I$, the identity matrix, and $F_{\underline{z}}$ the matrix of partial derivatives of the vector field $\dot{\underline{z}}=F(\underline{z},t)$, where $\underline{z}\equiv(x,y)\in\mathbf{T}\times\mathbf{R}$ and $t\in\mathbf{T}$. Then the required initial condition $(\delta x,\delta y)(0)=(\xi,\eta)$ is such that

$$M_{11}(t)\xi+M_{12}(t)\eta=0,$$

$$M_{11}(-t)\xi+M_{12}(-t)\eta=0.$$

There is a nonzero solution (ξ,η) iff

$$C(t)\equiv M_{11}(t)M_{12}(-t)-M_{12}(t)M_{11}(-t)=0.$$

Thus times $\pm t$ $(t>0)$ are conjugate iff $C(t)=0$. Computation of the forward and backward monodromy matrices provides even more information, however, namely if the initial condition is really on a rotational invariant torus then upper and lower bounds on its slope at the initial point can be obtained, more precisely a local Lipschitz cone. $C(t)=0$ corresponds to equality of the upper and lower bounds, and it follows that for larger t the upper bound is less than the lower bound, providing a contradiction to the existence of a rotational invariant torus through the initial point, so this approach was called the "cone-crossing criterion" in Ref. 11.

We explain briefly how to implement this version of the nonexistence criterion. It is done most conveniently by integrating the equation for the inverse monodromy matrix $N(t)=M(t)^{-1}$. Given an initial condition $\underline{z}_0$ at $t=0$, let $\underline{z}(\pm t,\underline{z}_0)$ be its forward and backward trajectories, and integrate

$$\dot{N}(t)=-N(t)F_{\underline{z}}(\underline{z}(t),t)\quad\text{with } N(0)=Id,$$

backwards and forwards in time (or just forwards if time-reversal symmetry can be used). Then for any $t>0$ let

$$w^{\pm}(t)=N(\mp t)\begin{pmatrix}0\\ \pm 1\end{pmatrix}=\begin{pmatrix}\pm N_{12}(\mp t)\\ \pm N_{22}(\mp t)\end{pmatrix},$$

which are tangent vectors at $\underline{z}_0$; they provide a local Lipschitz cone for any rotational invariant torus through the initial condition. Let $C(t)=w^{-}(t)\wedge w^{+}(t)$. Then $C(0)=0$ and $\dot{C}(0)>0$. If there is $t'>0$ such that $C(t')\leqslant 0$, then the orbit associated with $\underline{z}_0$ does not belong to an invariant rotational torus. In the time-reversible case with symmetric initial condition, then

$$w^{\pm}(t)=\begin{pmatrix}-N_{12}(t)\\ \pm N_{22}(t)\end{pmatrix}$$

and $C(t)=-2N_{12}(t)N_{22}(t)$. Although it is not an efficient way to compute $\delta x(t)$, note that for horizontal initial vector, $\delta x(t)=N_{22}(t)/\det N(t)$, and for vertical initial vector, $\delta x(t)=-N_{12}(t)/\det N(t)$ (and $\det N=1$ in the conservative case).

[1] G. D. Birkhoff, Acta Math. **43**, 1 (1922).
[2] A. Celletti, ZAMP **41**, 174 (1990).
[3] A. Celletti and L. Chierchia, "Quasi-periodic attractors in celestial mechanics," Arch. Ration. Mech. Anal. (to be published).
[4] A. Celletti, C. Froeschlé, and E. Lega, Planet. Space Sci. **55**, 889 (2007).
[5] A. C. M. Correia and J. Laskar, Nature (London) **429**, 848 (2004).
[6] C. Froeschlé, E. Lega, and R. Gonczi, Celest. Mech. Dyn. Astron. **67**, 41 (1997).
[7] P. Goldreich and S. Peale, Astron. J. **71**, 425 (2000).
[8] G. J. F. MacDonald, Rev. Geophys. **2**, 467 (1964).
[9] R. S. MacKay, Physica D **36**, 64 (1989).
[10] R. S. MacKay, J. D. Meiss, and J. Stark, Nonlinearity **2**, 555 (2000).
[11] R. S. MacKay and I. C. Percival, Commun. Math. Phys. **98**, 469 (1985).
[12] S. J. Peale, Icarus **178**, 4 (2005).
[13] J. Stark, Commun. Math. Phys. **117**, 177 (1988).
[14] H. Yoshida, Phys. Lett. A **150**, 262 (1990).
[15] M. Guzzo, E. Lega, and C. Froeschlé, Physica D **163**, 1 (2002).